National Renewable Energy Laboratory
Innovation for Our Energy Future

A national laboratory of the U.S. Department of Energy
Office of Energy Efficiency & Renewable Energy

Stability of CIS/CIGS Modules at the Outdoor Test Facility over Two Decades

Preprint

J.A. del Cueto, S. Rummel, B. Kroposki,
C. Osterwald, and A. Anderberg
National Renewable Energy Laboratory

Presented at the 33rd IEEE Photovoltaic Specialists Conference
San Diego, California
May 11–16, 2008

Conference Paper
NREL/CP-520-42541
May 2008

NREL is operated by Midwest Research Institute • Battelle Contract No. DE-AC36-99-GO10337

STABILITY OF CIS/CIGS MODULES AT THE OUTDOOR TEST FACILITY OVER TWO DECADES

J.A. del Cueto, S. Rummel, B. Kroposki, C. Osterwald, A. Anderberg
National Renewable Energy Laboratory (NREL), 1617 Cole Boulevard, Golden, CO 80401, USA

ABSTRACT

We examine the status and question of long-term stability of copper indium diselenide (CIS) photovoltaic (PV) module performance for numerous modules that are deployed in the array field, or on the roof of, the outdoor test facility (OTF) at NREL, acquired from two manufacturers. Performance is characterized with current-voltage (I-V) measurements obtained either at standard test conditions (STC) or under real-time monitoring conditions, taken over the course of many years. We present and scrutinize I-V characteristics for degradation modes. Analysis yields that CIS PV modules can exhibit either moderate (2% to 4% per year) to negligible or small (less than 1% per year) degradation rates, and that the predominant loss mode appears to be fill factor diminution, often associated with increases in the series resistance in some of the modules. A secondary mode of degradation observed comprises metastable changes to the open-circuit voltage. The featured modules are deployed on three separate testbeds.

INTRODUCTION

Currently, the highest performing thin-film PV devices are cells comprised of copper indium-gallium diselenide (CIGS) at approximately 19.9% [1]. The best efficiencies obtained from large area PV modules of this technology are about 11%–12%, as measured at standard test conditions (STC). However, the long-term stability of CIS/CIGS modules has become a key issue with this technology. Performances changes are observed in CIGS devices when subjected to damp-heat stress and/or illumination or bias as noted: decreases in open-circuit voltage(Voc) via changes in doping density and conduction band offsets between CIS absorber and cadmium sulfide (CdS) window layers [2]; losses in Voc due to defect-induced recombination and fill factor (FF) loss by type conversion at the CdS/CIGS interface brought about by degradation of the zinc oxide (ZnO) transparent conductive oxide (TCO) [3]; defects in and degradation of the ZnO and CdS layers, leading to poor conductivity or damage at the CdS/CIGS interface [4]; degradation of the top ZnO or CdS/CIGS interface [5] leading to series resistance increases and FF losses. Most of the studies cited have focused on unencapsulated CIGS devices.

EXPERIMENTAL PROCEDURE

Beginning in 1988 and continuing up until 2005, CIS modules from one manufacturer (A) were deployed at the OTF; and starting 2002, we began deploying CIS modules from a second manufacturer (B). We emphasize that the A modules are no longer manufactured or available, but we still retain many of them deployed at the OTF. All modules were baseline tested under STC using one or more of three solar simulator testbeds: the SPIRE pulsed-light source, the large-area continuous (LACSS) and the standard outdoor measurement (SOMS) systems. Afterwards, modules were deployed out in the field as: 1) single free-standing modules (A and B) on the long-term exposure rack, loaded with a fixed resistor across their terminals (whose value approximates the optimum load at STC); 2) single modules (A and B) deployed on the Performance and Energy Ratings Testbed (PERT) system on the roof of the OTF starting in 1997; and 3) an array of type A modules on the high-voltage stress testbed (HVST2) starting in 2005. Periodically, the long-term exposure and PERT modules were taken indoors for further measurements of I-V characteristics at STC. Module I-V power parameters (Voc, FF, etc.) measured at STC are subsequently scrutinized for changes against time.

PERT modules are connected to a data acquisition system (DAS) that performs I-V traces in situ once every 15 minutes, and at other times actively maintains the modules loaded at their optimum power point appropriate for the instantaneous lighting and temperature conditions. The HVST2 array comprises 24 thin-film CIGS modules deployed in two, bipolar strings of 12 modules connected in series, with nominally ±300 VDC open-circuit voltage and 1 kW total power. For this array, another DAS also performs I-V traces in situ on each of the strings periodically, or actively loads each string at instantaneous optimum-power-point conditions at other times. Additionally, the HVST2 DAS can be programmed to, and performs cyclic biasing of each string to fixed-voltage levels that are stepped over time to produce square-wave bias vs. time.

PERT and HVST2 modules are deployed at fixed, latitude tilt (40°) and face due south: these data comprise real-time outdoor measurements, executed with programmable electronic loads that trace the I-V characteristics. Also, we monitor and record irradiance with broadband pyranometers, plus air and module temperatures using type 'T' thermocouples. More detailed description of and analysis of PERT system and outdoor data were described elsewhere [6]. In this paper, we narrow our focus of real-time PERT and HVST2 data to that obtained within fixed irradiance windows, and perform corrections of the I-V power parameters to reference temperature (25°C) by least-squares fitting thereof to linear temperature dependence scrutinized and calculated within 30-day intervals. Furthermore, for the HVST2 array, we present the power performance rating calculated monthly according to PVUSA Test Conditions (PTC) regression analysis [7].

The STC data measured on the LACSS were further analyzed by normalizing the module voltages and currents to the unit cell level, achieved by: dividing the module voltage (V) by the number of series-connected cells, and current to current density (J) by dividing by the area of each unit cell (taken as the module aperture area divided by the number of cells). These cell areas are approximately 10%–15% larger than the active area —so J data are correspondingly smaller—due to interconnect and border area losses extant in modules. Device level parameters like the series resistances, diode quality factors (A), reverse saturation current density (J_0), and shunt conductance (Gsh) values are derived via standard diode analysis as shown in the literature [8]: e.g., series resistance data are derived from the intercept of the locus of slopes of the J-V data (dV/dJ) vs. J, extrapolated to the origin with 1/J (for dark) or 1/(J+J_{Light}) (for light) characteristics.

DATA AND ANALYSIS

Long-Term Outdoor Testbed

Figure 1 is a composite graph depicting the I-V power parameters measured predominantly on the SPIRE at STC for modules on the long-term exposure rack: the efficiency, FF, Voc and Isc data are shown, respectively, at bottom, second-from-bottom, second-from-top, and the top panes in the graph, plotted vs. time; for the A modules deployed beginning in 1988, and starting in 2002 for the B modules. The abscissae for the Isc and Voc panes in Fig. 1 comprise changes in scale in order to depict disparate current and voltages. Also depicted are: an A module (orange) deployed on PERT and tested indoors occasionally beginning in 1997, and a B module also deployed on PERT. The A modules represent five separate vintages of CIS technology ranging 1988 to 1998. The initial efficiency values for the A modules are about 8% in 1988, improving over time up to 11%–12%; initial B module efficiency are about 11%. The efficiency data of A modules from 1990–1992 vintages appear stable, but later-vintage A module data are less stable. One of the 1988 A modules was removed and returned to manufacturer in 1998 after dropping to ~6%, but a second one has held up better, undergoing a cumulative change in efficiency from about 8% to 5.9% over a 20-year period, or equivalently 1.3% relative loss per year. Furthermore, Fig. 1 depicts some of the difficulties encountered in accurate testing methodology at STC over the long-term: in 1990 a hardware revision altered the data abruptly for the 1988 A modules, resulting in a sharp drop of 0.5% in efficiency, without which the loss rate would be only 1.0% per year (%/yr). The relative performance loss rates for the modules shown in Fig. 1 range from negligible for 1990 A modules, up to -2.2%/yr for the 1998 A modules. For the 1997 A module depicted in Fig. 1—resident of the PERT—there appears transient improvement, about 10%-relative between tests conducted in 2006 and 2007: during this time the module lay indoors under low light levels and room temperature, while the PERT system was re-wired. Some of this transient behavior also appears in the PERT data shown later.

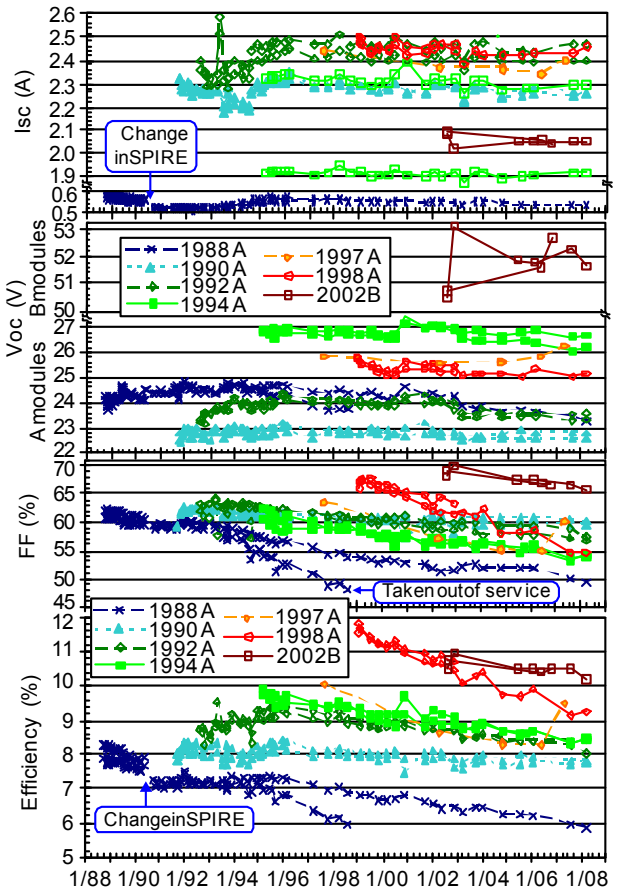

Figure 1. CIS/CIGS A and B module efficiency, FF, Voc, and Isc data, respectively, at bottom, second-from-bottom, second-from-top, and top panes, measured indoor at STC, plotted against time from 1988 up to 2008.

Although it may be early to conclude definitively based on six years of data, the B modules in Fig. 1 appear more stable, exhibiting a cumulative loss of less than 0.5% absolute, less than 1%/yr relative loss rate. Fig. 1 shows the primary mode of degradation for A modules is FF loss, followed by some Voc decline. However, note that Voc appears to exhibit slight improvement after the initial few years of deployment for the A modules of vintages made on or before 1992, followed by subsequent loss afterwards. Similarly for B modules, there is some FF loss with time, plus transient and slight improvement in Voc initially after deployment.

Losses in FF are scrutinized for select A and B modules, by deriving and analyzing the slopes (dV/dJ, 3-point) of the dark and light J-V characteristics, for information on series resistance and shunt conductance. These data are depicted in composite, multi-pane graphs, Figs. 2 and 3, respectively, for 1988 A and 1994 A modules, and 1998 A and 2002 B modules. In both Figs. 2 and 3, the slopes (dV/dJ) are read along the left-hand abscissae, their dependence plotted against 1/J along the ordinate at the bottom in the case of the dark J-V data, or plotted against 1/(J + J_{Light}) along the upper ordinate (in reverse order) for

the light J-V data. The units of the ordinate axes are inverse amps per square centimeter (cm^2/A); for the abscissae they are ohm-cm^2. The values of J_{Light} used are the measured short-circuit current density (Jsc). The top and bottom panes in each graph portray: the data for 1988 A and 1994 A modules, respectively, in Fig. 2; and in Fig. 3, the data for 2002 B and 1998 A modules, respectively. The series resistance are derived from extrapolation of the locus of slopes to the origin 1/J or $1/(J+J_{Light})$. In the figure legends, 'Drk' or 'Lit' refer, respectively, to dark or light J-V data; and the two-digit numbers (e.g., 99, 02, 05, 07, 08) denote the year the measurements were taken to show how the series resistance values have evolved with time.

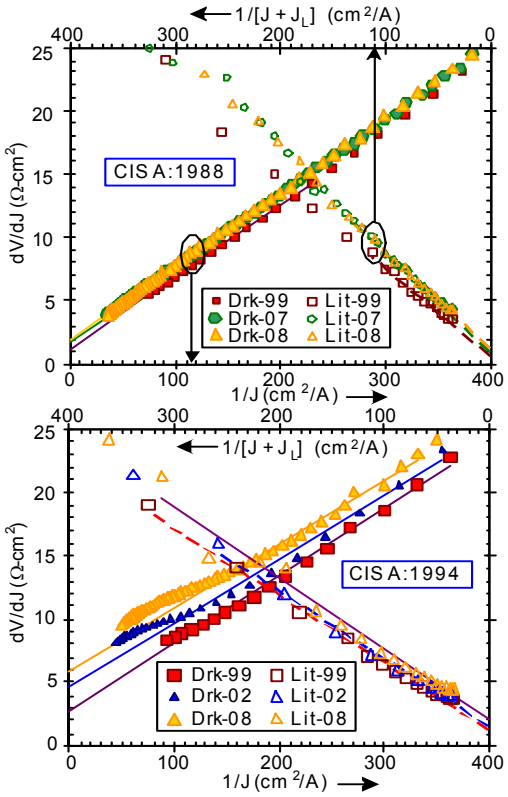

Figure 2. Slopes dV/dJ for 1988 A and 1994 A modules, respectively, in top and bottom panes, plotted vs. 1/J for dark J-V data read along lower ordinate, and $1/(J+J_L)$ for light J-V data, read along upper ordinate axes.

From the top pane in Fig. 2, we observe that the series resistance of the 1988 A module has changed only slightly between 1999 and 2008, by about 1 ohm-cm^2 for dark data and somewhat less for the light data. Conversely, for the 1994 A module in the lower pane, the dark J-V slopes are more appreciably shifted upwards, indicating an increase of about 3 ohm-cm^2, somewhat less than ~1 ohm-cm^2 for light J-V slopes, evolving over time for curves taken in 1999, 2002 and 2008. Also note that for the 1994 A module, the dV/dJ data exhibit non-linear behavior in far forward bias in the dark, that may be indicative of the development and appearance of a reverse-bias barrier [8] for the device in the dark, whose effect however, diminishes in the light. Similarly, the top-most pane in Fig. 3 indicates non-linear characteristics for the 2002 B module, an effect that appears to exacerbate with time (2002 to 2008) for the dark dV/dJ data, but to lesser extent in the light. This curvature for the 2002 B data complicates the analysis, albeit, note that even though the slope of the characteristics (dV/dJ–1/J) get steeper, the intercept values with the origin do not appear to alter significantly with time, indicating that the changes are not likely due to series resistance. For the 1998 A module in the bottom pane of Fig. 3, we observe substantial increases in series resistance values over time, about 4 ohm-cm^2 and 1–2 ohm-cm^2, respectively, for dark and light data. We emphasize that because Jsc values are notably larger for the A modules (30 mA/cm^2) than for the B modules (24 mA/cm^2), that even with comparable series resistance, the A module performance will be impacted more adversely.

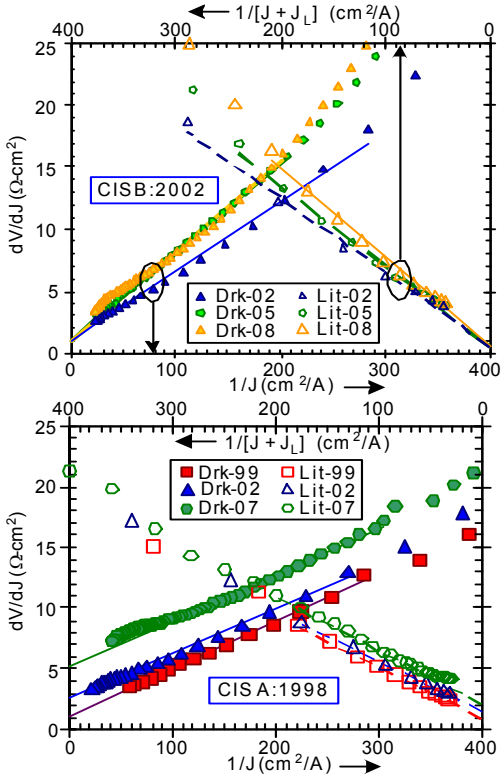

Figure 3. Slopes dV/dJ for 2002 B and 1998 A modules, respectively, in top and at bottom panes, plotted vs. 1/J for dark J-V data read along lower ordinate, and $1/(J+J_L)$ for light J-V data, read along upper ordinate axes.

Determination of Gsh values from typical J-V curves is illustrated in Fig. 4: in upper and lower panes, respectively, depicting the slopes dJ/dV near zero bias, for the 2002 B and 1998 A modules, measured over the course of several years (e.g., 1999, 2002, 2008, etc.) in the dark at 25°C temperature. The units shown for the slopes are milliSiemens per cm^2 (mS/cm^2), reduced to unit area cell level. We take the value of Gsh to be the minimum of the locus of the slopes against bias, which typically occurs at

zero or in slight reverse bias. We point out that we tend to minimize the reverse bias voltage employed in the J-V measurements in order to minimize the risk of damaging the modules. From Fig. 4, we see that the shunt has been slowly increasing for the 2002 B module, from 0.2 mS/cm^2 in 2002 up to ~ 0.55 mS/cm^2 in 2008; whereas it has remained fairly low for the 1998 A module, at or less than 0.2 mS/cm^2. Although the increase for the 2002 B appears significant, even at the 2008 level (0.55 mS/cm^2), it has a small impact on the reduction of the optimum-point current and FF at 1-sun illumination, albeit it is just above the 1% level. Where it has a larger impact on relative loss is at low light levels. For the 1998 A module, the shunt has negligible effect on performance loss. We point out that the derived series resistance and shunt values can be and are subsequently used to correct the apparent measured voltages for series resistance effects and observed current for parasitic shunt conductance in order to extract diode quality (A) and J_0 data from the J-V curves [8].

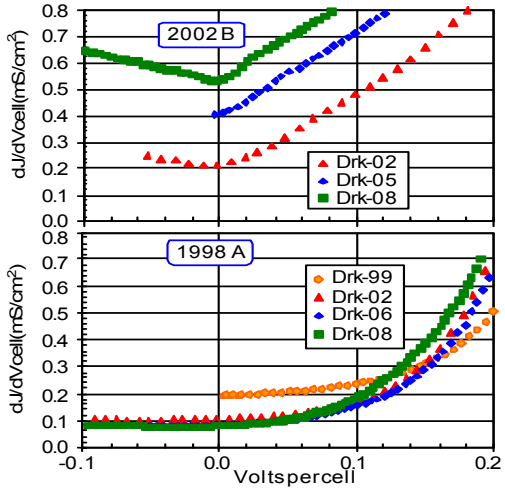

Figure 4. Shunt conductance (Gsh) determination from the slopes (dJ/dV) near zero bias for 1998 A and 2002 B modules, respectively, shown in lower and upper panes, vs. voltage per cell between –0.1 V and +0.2 V.

High Voltage Stress Testbed Array

In Fig. 5, we show the monthly rated power for each of the positive (+) and negative (–) strings of the HVST2 array, using the PTC ratings method, plotted against time from Feb. 2005 up till March 2008. Both strings appear to be experiencing a moderate decline in rated power. The relative power loss rate for the negative string appears significantly larger ~ -3.8%/yr than that of the positive string at -2.55%/yr. Each string's losses are further scrutinized via the I-V power parameters illustrated in Fig. 6.

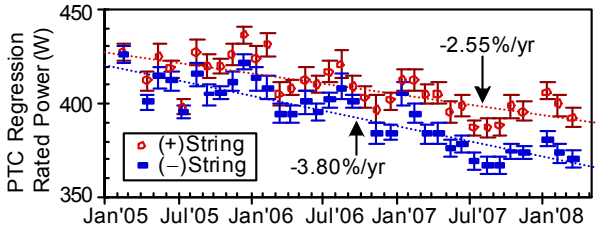

Figure 5. HVST2 CIGS A module bipolar string array power at rated PVUSA Test Conditions (PTC) vs. time.

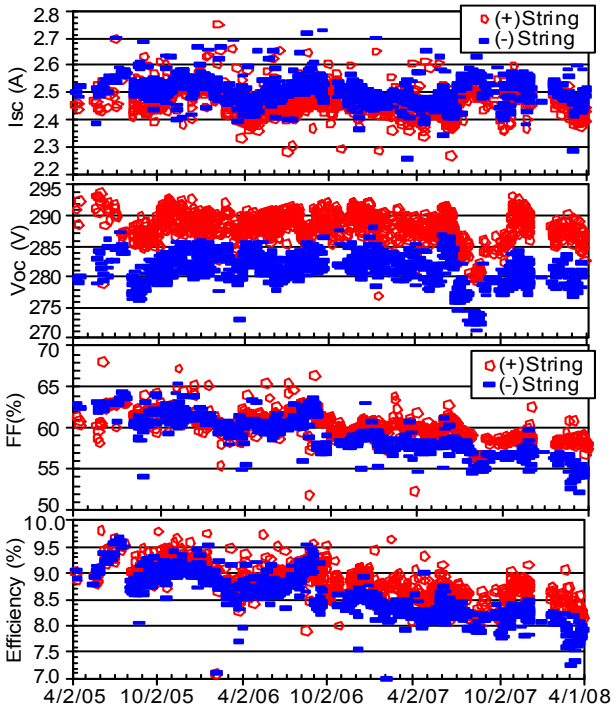

Figure 6. HVST2 array strings' Isc, Voc, FF, and efficiency data, respectively, at top, second-from-top, second-from-bottom, and bottom panes, within 1000 ±25 W/m^2 irradiance, corrected to 25°C temperature, plotted vs. time.

Figure 6 is a composite graph depicting the I-V power parameters for each string of the array, taken from I-V traces measured outdoors within a narrow band of irradiance levels, 1000 ±25 W/m^2, under predominantly clear-sky conditions, corrected to reference temperature (25°C). The efficiency, FF, Voc and Isc data are shown, respectively, in the bottom, second-from-bottom, second-from-top, and top panes of the graph, plotted vs. time from April 2005 to March 2008. The efficiency are calculated by dividing the power from each string by the irradiance incident on the sum aperture areas of the 12 modules in each string. Fig. 6 indicates that FF losses are largely responsible for the performance losses in each of the array's strings, dropping from about 62.5% to 58.5%, and 63% down to 55.6%, respectively, for the positive and negative strings, over the three-year period; or equivalently a loss rate of -2.1%/yr and -4.0%/yr, respectively, for positive and negative strings. The Voc data for the negative string are overall lower by about 7 volts than for the positive string; and exhibit slight degradation loss rates, -0.3%/yr and -0.2%/yr, respectively, for the negative and positive strings, whose sizes are larger than the 95% statistical significance level (~ ±0.04%/yr). The overall loss rates in performance are -2.9%/yr and -4.7%/yr, respectively, for the

positive and negative strings at 1000 W/m^2, rates that are slightly larger than the power loss rates obtained from the PTC regression analysis portrayed in Fig. 5.

PERT System

The I-V power parameters for a 1997 A and 2002 B module are portrayed, respectively, in Figures 7 and 8, using data taken outdoors under predominantly clear-sky conditions with a DAS, focusing on two narrow bands of irradiance at 1000 ±25 W/m^2 and 500 ±25 W/m^2. The data are corrected to 25°C temperature. Additionally, the Isc data are normalized to the center of each respective illumination level, but are not spectrally corrected. Each figure comprises a multi-pane graph depicting the Isc, Voc, FF, and efficiency data, respectively, in the top, second-from-top, second-from-bottom, and bottom panes, plotted vs. time from Jan. 2002 to Dec. 2007. There are two notable gaps in these data: during 2005 when the modules were deployed and biased at peak-power but no I-V traces were taken, and from mid-2006 to mid-2007, when the PERT was re-wired, during which time the modules were stored indoors.

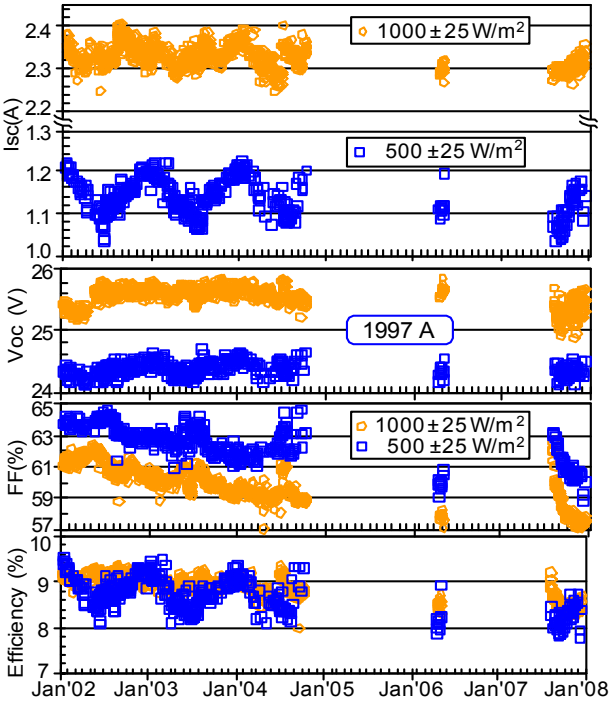

Figure 7. 1997 A module Isc, Voc, FF, and efficiency data, respectively, at top, second-from-top, second-from-bottom, and bottom panes, at 1000 W/m^2 and 500 W/m^2 irradiance, corrected to 25°C temperature plotted vs. time.

A salient feature derived from these two figures is that the primary source of performance decline for each module appears dominated by FF degradation. Another notable feature is the appearance of transient behavior: in FF data for the 1997 A module, and increases in Voc for the 2002 B module (~2 volts at 1000 W/m^2), both observed just after re-deployment in 2007. The 2002 B module Voc data show transient increase just after initial deployment in 2002 as well. For the 1997 A module, the FF data appear elevated above the long-term trend line by 4%-absolute after re-deployment in Aug. 2007, to nearly identical values as it had in Jan. 2002. None of the transitory changes in the 1997 A FF data are temperature related, as these data are temperature corrected, and if anything, the changes in uncorrected FF data are even more prominent.

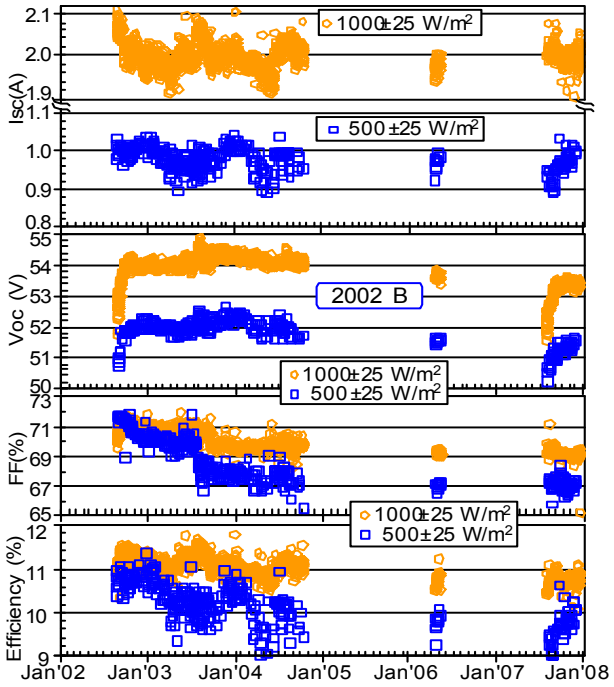

Figure 8. 2002 B module Isc, Voc, FF, and efficiency data, respectively, at top, second-from-top, second-from-bottom, and bottom panes, at 1000 W/m^2 and 500 W/m^2 irradiance, corrected to 25°C temperature plotted vs. time.

We note the contrasting behavior in FF data as time progresses: for the 1997 A module, data at 1000 W/m^2 are offset to lower values compared to data at 500 W/m^2 by ~3%-absolute, degradation in both irradiance bands appears to occur in tandem at a rate of about -0.7%/yr; for the 2002 B module, data in each illumination window start out at comparable values, but subsequently, the data at 500 W/m^2 decline more rapidly (-0.9%/yr) than that at 1000 W/m^2 (-0.5%/yr). The FF degradation rates at the two illumination levels appear consistent with series-resistance dominated losses for the 1997 A module, and shunt-related losses in the 2002 B module. Finally, we note the largest uncompensated variations in efficiency depicted in Figs. 7 and 8 are driven by seasonal fluctuations in Isc, that albeit are temperature-corrected, are larger for data at the lower irradiance than at high irradiance; and surmise these are driven by a combination of cyclic cosine response to angle-of-incidence and air mass oscillations, both of which attain their respective high values during the winter, lows in summertime, and whose variations are larger for data at 500 W/m^2 irradiance.

SUMMARY AND CONCLUSIONS

The degradation rates for the various CIS/CIGS modules studied under the test conditions referenced are listed in table 1, with mean loss rates and their 95% statistical confidence levels listed, respectively, in the second and third columns from the left. The first 10 rows, below the top, comprise modules strictly tested at STC, residents of the long-term exposure testbed. The next populated six rows comprise the PERT system modules; and last four rows represent the HVST2 array positive and negative string module data. For the PERT modules, tests at STC as well as real-time data measured in situ within the 500 W/m^2 and 1000 W/m^2 irradiance bands are listed. For the HVST2 array, we present the degradation measured in situ at 1000 W/m^2, and from the PTC-regression-rating analysis, respectively, in the last four rows. For example: for the 1988 A module, the calculated loss rate is -0.90 ±0.13 %/yr, with 95% confidence, during the time between November 1990 and March 2008, as gauged at STC indoors; for the 2002 B module on PERT, the loss rate measured at STC indoors between 2002 and 2006, is -0.65 ±3.3 %/yr, which does not appear significant, but however, for the same module, the in-situ PERT data measured outdoor between 2002 and 2007 at 1000 W/m^2 indicates a loss rate of -0.89 ±0.04 %/yr, which is statistically significant. Some of this ambiguity is due to FF declines that are partly offset by increases in Voc or Isc.

Table 1. Summary of Performance Degradation Rates

Module Type	ΔEff/Eff$_0$ (%/yr)	95% (%/yr)	TEST CONDITION	TIMELINE
1988 A	-0.90	0.13	STC	Nov-90 –Mar-08
1990 A	-0.21	0.10	STC	Oct-91–Mar-08
1990 A	-0.32	0.12	STC	Oct-91–Mar-08
1992 A	-0.43	0.22	STC	Aug-92–Mar-08
1992 A	-0.43	0.18	STC	Aug-92–Mar-08
1994 A	-1.08	0.14	STC	Mar-95–Mar-08
1994 A	-0.95	0.17	STC	Mar-95–Mar-08
1998 A	-2.25	0.23	STC	Jan-99–Mar-08
1998 A	-2.14	0.56	STC	Jan-99–Nov-02
2002 B	-0.69	0.96	STC	Aug-02–Mar-08
1997 A	-2.10	1.06	STC (PERT)	Aug-97–May-07
1997 A	-1.35	0.14	500 PERT	Jan-02–Dec-07
1997 A	-1.27	0.04	1000 PERT	Jan-02–Dec-07
2002 B	-0.65	3.30	STC (PERT)	Aug-02–Oct-06
2002 B	-1.80	0.16	500 PERT	Aug-02–Dec-07
2002 B	-0.89	0.14	1000 PERT	Aug-02–Dec-07
2004 A	-2.87	0.15	1000 HVST2 POS. STR.	Apr-05–Mar-08
2004 A	-4.68	0.15	1000 HVST2 NEG. STR.	Apr-05 –Mar-08
2004 A	-2.55	0.86	PTC HVST2 POS. STR.	Apr-05–Mar-08
2004 A	-3.77	0.82	PTC HVST2 NEG. STR.	Apr-05 –Mar-08

We assert that for some modules, notably the 1990 A and 1992 A modules, the degradation rates are quite low—ranging -0.2%/yr to -0.4%/yr—even though the individual FF loss rates are higher, because they're offset by positive changes in Voc. This happens to some degree as well for the 2002 B modules measured at STC. Furthermore, from STC data, the primary loss mechanism for the A modules appears to be dominated by series resistance increases, further exacerbated by their high Jsc. We also note that moderately higher degradation rates are observed for the 2004 A modules on the high-voltage array, between -2.5%/yr and -4.7%/yr, with the highest loss rate incurred by the negatively biased string.

For the B modules measured indoors at STC, the overall loss rates appear statistically insignificant, albeit there exists a substantial FF loss mode—3% to 5%—whose source is complicated: predicated by a combination of shunt conductance and/or apparent diode quality factor increases. The shunt conductance increases in these by a factor of 3–5, but can only be partly responsible for the FF loss, that may appear as increases in diode quality factor, but under closer scrutiny looks more like changes in a two-diode device model, with the primary diode weakening, as indicated by increases in J_0.

ACKNOWLEDGEMENTS

This work was supported by the U.S. Department of Energy under Contract No. DE-AC36-99GO10337. I thank Ingrid Repins and Keith Emery at NREL for their timely and valuable editorial comments on this paper

REFERENCES

[1] I Repins, M A Contreras, B Egass C DeHart, J Scharf, C L Perkins, B To, R Noufi, "19.9%-efficient ZnO/CdS/CuInGaSe2 Solar Cell with 81.2% Fill Factor," Prog. in PV: Res. & Appl. **16**, 2008, pp. 235–239.

[2] C Deibel, V Dyakonov, J Parisi, J Palm, S Zweigart, F Karg, "Influence of damp heat testing on the electrical characteristics of Cu(In,Ga)(S,Se)2 solar cells," Thin Solid Films, **403-404**, 2002, pp. 325–330

[3] M Schmidt, D Braunger, R Schaffler, H W Schock, U Rau, "Influence of damp heat on the electrical properties of Cu(In,Ga)Se2 solar cells," Thin Solid Films **361-362**, 2000, 283–287

[4] G A Medvedkin, E I Terukov, Y Hasegawa, K Hirose, K Sato, "Microdefects and point defects optically detected in Cu(In,Ga)Se2 thin film solar cells exposed to damp and heating," Sol. Ener. Mats & Sol. Cells **75,** 2003, pp. 127–133.

[5] J Wennerberg, J Kessler, M Bodegard, L Stolt, "Damp Heat Testing of High Performance CIGS Thin Film Solar Cells," Proc. 2nd WCPEC (1998), Vienna, pp. 1161–1164.

[6] J A del Cueto, "Review of the Field Performance of One Cadmium Telluride Module," Prog. In PV: Res. & Appl., **6**, 1998, pp. 433–446.

[7] C M Whitaker, T U Townsend, "Application and Validation of a New PV Performance Characterization-Method," Proc. 26th IEEE PVSC, 1997, p.1253–1256.

[8] Hegedus SS, Shafarman WN. Thin-Film Solar Cells: Device Measurements and Analysis. Progress in PV: Res. & Appl. **12**: 2004; pp. 155–176.

REPORT DOCUMENTATION PAGE

Form Approved
OMB No. 0704-0188

PLEASE DO NOT RETURN YOUR FORM TO THE ABOVE ORGANIZATION.

1. REPORT DATE *(DD-MM-YYYY)*	2. REPORT TYPE	3. DATES COVERED *(From - To)*
May 2008	Conference Paper	11-16 May 2008

4. TITLE AND SUBTITLE
Stability of CIS/CIGS Modules at the Outdoor Test Facility over Two Decades: Preprint

5a. CONTRACT NUMBER
DE-AC36-99-GO10337

5b. GRANT NUMBER

5c. PROGRAM ELEMENT NUMBER

6. AUTHOR(S)
J.A. del Cueto, S. Rummel, B. Kroposki, C. Osterwald, and A. Anderberg

5d. PROJECT NUMBER
NREL/CP-520-42541

5e. TASK NUMBER
PVB77101

5f. WORK UNIT NUMBER

7. PERFORMING ORGANIZATION NAME(S) AND ADDRESS(ES)
National Renewable Energy Laboratory
1617 Cole Blvd.
Golden, CO 80401-3393

8. PERFORMING ORGANIZATION REPORT NUMBER
NREL/CP-520-42541

9. SPONSORING/MONITORING AGENCY NAME(S) AND ADDRESS(ES)

10. SPONSOR/MONITOR'S ACRONYM(S)
NREL

11. SPONSORING/MONITORING AGENCY REPORT NUMBER

12. DISTRIBUTION AVAILABILITY STATEMENT
National Technical Information Service
U.S. Department of Commerce
5285 Port Royal Road
Springfield, VA 22161

13. SUPPLEMENTARY NOTES

14. ABSTRACT *(Maximum 200 Words)*

We examine the status and question of long-term stability of copper indium diselenide (CIS) photovoltaic (PV) module performance for numerous modules that are deployed in the array field, or on the roof of, the outdoor test facility (OTF) at NREL, acquired from two manufacturers. Performance is characterized with current-voltage (I-V) measurements obtained either at standard test conditions (STC) or under real-time monitoring conditions, taken over the course of many years. We present and scrutinize I-V characteristics for degradation modes. Analysis yields that CIS PV modules can exhibit either moderate (2% to 4% per year) to negligible or small (less than 1% per year) degradation rates, and that the predominant loss mode appears to be fill factor diminution, often associated with increases in the series resistance in some of the modules. A secondary mode of degradation observed comprises metastable changes to the open-circuit voltage. The featured modules are deployed on three separate testbeds.

15. SUBJECT TERMS
PV; copper indium diselenide; photovoltaic; module; current-voltage; open-circuit voltage; short-circuit current; electronic loads.

16. SECURITY CLASSIFICATION OF:			17. LIMITATION OF ABSTRACT	18. NUMBER OF PAGES	19a. NAME OF RESPONSIBLE PERSON
a. REPORT	b. ABSTRACT	c. THIS PAGE			
Unclassified	Unclassified	Unclassified	UL		19b. TELEPHONE NUMBER (*Include area code*)